IEEE Access
Multidisciplinary : Rapid Review : Open Access Journal

Received 13 October 2022, accepted 26 October 2022, date of publication 28 October 2022, date of current version 8 November 2022.

Digital Object Identifier 10.1109/ACCESS.2022.3218047

RESEARCH ARTICLE

Investigation on the Physical Properties of Varistors According to Temperature

AHRAN MIN, SIN-DONG KANG, AND JAE-HO KIM
Department of Fire and Disaster Prevention Engineering, Daejeon University, Daejeon 34520, South Korea

Corresponding author: Jae-Ho Kim (jkim@dju.ac.kr)

This work was supported by the Daejeon University Grants (2022).

ABSTRACT This study aims to determine the basic physical properties of varistor, which is a protective element in a surge protection device (SPD) used to prevent damage to electric and electronic equipment due to lightning. To do this, we conducted tests of insulation resistance, leakage current, heating characteristics, accelerated aging, impulse current, and operating duty according to temperature. To measure insulation resistance and leakage current, an S1-1568 insulation resistance tester was used. To measure the temperature rise according to a change in the external environment, a convection oven was employed. For the impulse current test, a surge current generator of a direct lightning strike, which was designed and manufactured according to the IEEE and UL standards, was used. We verified that the leakage current increased and the insulation resistance decreased as the voltage and outside temperature were applied to the varistor. This meant that heating and deterioration accelerated due to the leakage current, depending on the place where the SPD was applied. Heat accumulation due to constant heating could cause a change in the physical properties of a varistor and degradation of performance, leading to failure. The impulse current test results of the varistor through the operating duty test showed that changes in insulation resistance and leakage current did not occur significantly with an increase in the number of impulse applications when the less than the maximum surge currents. On the other hand, the maximum surge current was exceeded, the insulation resistance rapidly decreased, which also rapidly increased the leakage current.

INDEX TERMS SPD, MOV, varistor, surge protection device.

I. INTRODUCTION

With the increase in fossil fuel usage after the 19th century's Industrial Revolution, the emission of greenhouse gases, such as carbon dioxide, has also rapidly increased. As a result, global warming and climate change have accelerated. Accordingly, the frequency of torrential rains, along with lightning flashes to the earth in summer, has also increased with damage [1]. IEC 62305 - 1 defines lightning flash to earth as an electrical discharge of atmospheric origin between the cloud and the earth, consisting of one or more strokes [2]. When lightning flash to earth strikes buildings and surrounding lead-in wires, and it can also be a cause to induce damage to electric and electronic devices as well as lead to fires and explosions [3].

The associate editor coordinating the review of this manuscript and approving it for publication was Fabio Mottola.

A surge is a transient phenomenon that occurs by lightning electromagnetic impulses as a result of overvoltage or overcurrent, which generates a high voltage of hundreds to thousands of volts instantaneously, thereby destroying a variety of electronic devices. According to the Lightning Yearbook of the Korea Meteorological Administration in 2020, the average number of lightning flashes to the earth per year in the inland area of South Korea over the last 10 years has been 117,681 times. According to the National Fire Data System at the Nation Fire Agency, 160 cases of property damage due to lightning flashes have occurred, and eight persons have been injured in the last 10 years. As for the type of damage due to lightning, failures of electric and electronic devices accounted for the largest proportion, followed by fires (32%), outages (8%), and human casualties (2%) [4]. Accordingly, international standards on lightning protection and electric equipment have continued to study efficient and safe energy uses, and industries, such as the petrochemical industry, have recommended using an improved lightning protection system [5].

To prevent damage caused by lightning strikes on buildings, lightning protection systems are installed, both external and internal [6]. An external lightning protection system is installed in the structure to be protected. It consists of an air-termination system, a down conductor system, and an earth-termination system to discharge lightning current from the point of a strike to the ground. An air-termination system induces a direct lightning strike. Down conductor and earth-termination systems play a role in flowing a lightning stroke current into a ground electrode and discharging the lightning current to the earth, respectively. An internal lightning protection system is installed to prevent flashover caused by a lightning current that flows through the conductive portion of an external lightning protection system and the structures to be protected from lightning. In it, a bonding conductor and a surge protective device are installed to reduce the electronic impact of the lightning stroke current. The distribution of the lightning stroke current is calculated according to IEC 62305 - 1. Generally, 50% is discharged to grounding equipment when a lightning stroke current is introduced into a building, and 50% is discharged to the grounding systems of other buildings or transformers through a surge protection device (SPD) and a low-voltage power line inside the building [2], [6], [7], [8]. As a result, burnout is more likely to occur in indoor and outdoor electric and electronic equipment due to the introduction of lightning stroke current through the lead-in wires rather than the damage to structures caused by direct lightning.

In some cases of damage that occurred due to lightning flash to earth, a ceiling in the machine room in an elevator was destroyed, and hikers were struck by a direct lightning strike on Bukhansan on July 29, 2007, resulting in death and casualties [9]. The survey results of 49,949 educational facilities across South Korea from 2015 to 2019 revealed that lightning damaged 982 facilities in five years, accounting for 2%. The largest portion of the damage came from cooling and heating equipment (358 cases), followed by firefighting equipment (351 cases), CCTV (300 cases), broadcasting equipment (188 cases), elevators (91 cases), and photovoltaic equipment (15 cases). To prevent this, much attention has been paid to the installation of the SPD, which is an internal lightning protection facility. However, around 21.1% (10,509 places) had external lightning protection systems, whereas only 6.2% had internal lightning protection systems, and only 2.5% had all protection facilities, including bonding [10].

An SPD is a device installed in a power supply and communication systems to protect electric and electronic devices from surges. It plays the role of an insulation circuit at nor-mal states, but when a surge current is introduced by a lightning stroke, it changes into a short circuit, discharging the surge current to the earth [11], [12], [13]. However, a leakage current may increase due to the deterioration or failure of SPD protective elements even if no surge is introduced, and if the heat protection function does not work correctly, it can lead to a thermal runaway [14], [15]. A thermal runaway is defined in IEC 61643 - 12 as an operating condition in which the power consumed inside the SPD exceeds the thermal dissipation capability of the connecting terminal, thereby increasing the temperature of the internal elements and ultimately resulting in an SPD failure [16], [17]. One of the telecommunication service providers in Korea had many cases of damaged wireless equipment due to lightning. As a result, SPD thermal runaways occurred, burning the SPD and making a fire in the main service panel of the base station [18]. A protective element in an SPD deteriorates over a long or short period through the absorption and discharge of surge voltage and current, thus increasing the leakage current and generating Joule heat. Here, a heat protection function works to prevent a thermal runaway. It is impossible to predict the status of SPD deterioration caused by the above conditions, which is a limitation of checking status through continuous on-site inspections.

Recently, there has been increased interest for damage of MOV caused by lightning strike. Zhang et al. have studied the lightning thermal damage characteristics of ZnO varistor under operating duty test [19]. He et al. conducted the withstand performance of SPD varistor under multi-pulse currents [20]. When the resistive leakage current increases, the third harmonic current also increases. Thus, a study on the diagnosis of the deterioration status of SPD using this characteristic has been conducted, but it lacks a proposal of the criteria of deterioration and failure [21].

As general methods to determine replacement time due to deterioration, the fault diagnosis method, surge counting method, and temperature measuring method are used [22]. A fault diagnosis method monitors the status of connecting fuses inside the SPD and indicates their status using a light-emitting diode. A surge counting method detects the number of surge inflows using a voltage divider. If the number exceeds a certain count, it recommends the replacement of the SPD. A temperature-measuring method measures the surface temperature of semiconductor devices inside the SPD, thereby determining deterioration if the temperature exceeds a certain temperature. However, few studies have been conducted on how to determine the deterioration status of SPD protection elements and the thermal runaway phenomenon from an engineering viewpoint. Thus, this study aimed to analyze physical properties according to external environmental changes, impulse currents, and thermal stability tests to determine the level of deterioration of varistor, which is an SPD protection element.

II. PHYSICAL PROPERTIES OF METAL OXIDE VARISTOR

A varistor is a nonlinear semiconductor device that suppresses surge voltage, converts surge current, and has a nonlinear current–voltage characteristic. If a varistor voltage (V_N) or lower is applied to a circuit, the varistor plays a role as an insulator. However, if a V_N or higher is applied to a circuit, it plays a role as a conductor, thereby classifying or

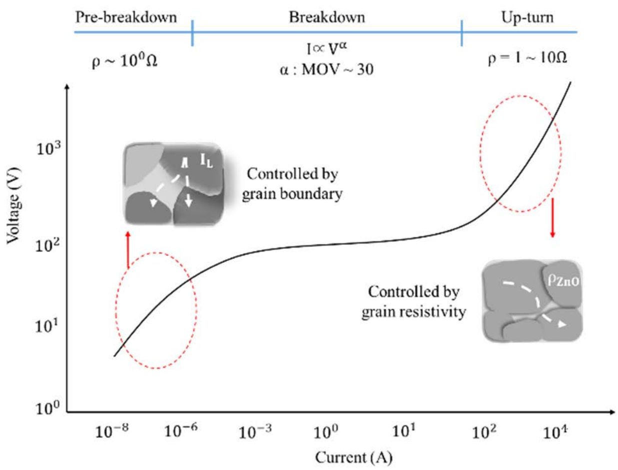

FIGURE 1. Characteristics of varistor: voltage-current curve.

FIGURE 2. SPD damaged by thermal runaway.

absorbing an overvoltage. As shown in Figure 1, the varistor current–voltage characteristic has a symmetric curve, which shows decreasing resistance when the voltage increases. The current–voltage characteristic graph has pre-breakdown, breakdown, and upturn regions [23]. The current–voltage characteristic is linearly exhibited in the pre-breakdown region, which is a low-voltage region. In the breakdown region, resistance rapidly drops, and a large current flows when an abnormal voltage is applied, resulting in a nonlinear shape of voltage and current.

The starting point in the breakdown region refers to the point at which the varistor element plays a role, from an insulator to a conductor, for an external voltage, which is defined as a $V_{\mathbf{N}}$. A $V_{\mathbf{N}}$ is the voltage applied to both ends of the varistor element when applying a direct current (DC) of 1 mA. In the upturn region, the current–voltage characteristic linearly changes when the current rapidly increases as the applied voltage increases. Due to the physical properties of a varistor, we expect it to have various types of impacts according to the system applied. A varistor forms a complex microstructure due to its uniform zinc oxide (ZnO) crystals and various additives. The size of the ZnO grain is around 20 - 30 μm, and the thickness of the depletion layer, which is the grain boundary, is around 10 – 100 nm. The resistance value of the ZnO grain is relatively small, whereas the resistance in the grain boundary is high. Thus, it has an electrical conduction mechanism in which a current flows in the direction where the grain boundary is small. A ZnO varistor has a 2 - 4 V breakdown voltage per intergranular barrier. If a uniform grain boundary potential barrier is not formed, a breakdown occurs in a place where the barrier is low, and the reliability of the varistor is significantly degraded [24], [25], [26]. If surge energy is repeatedly absorbed in a varistor, a vulnerable portion of the grain is destroyed, thereby degrading its performance. According to Table 4 - the general pass criteria of the design test in IEC 61643 - 11: a resistive current should not exceed 1 mA or should not vary more than 20% of the initial value set in the related test sequence. If this value is exceeded, we determine that a lifetime is degraded. If a varistor whose lifetime is degraded is used continuously, the leakage current increases inside the varistor, thereby generating heat accumulation due to heating and leading to an explosion or fire caused by a thermal runaway if the heat dissipation limit is exceeded. Figure 2 shows the SPD damaged by the thermal runaway caused by the generation of leakage current.

III. FUNDAMENTAL CHARACTERISTICS OF THE VARISTOR

To analyze the fundamental physical properties of the varistor, changes in leakage current and insulation resistance were measured using an S1 - 1568 insulation resistance tester. The selected test sample of the varistor was TVR - 14471 manufactured by Thinking Electronic Industrial Co. Ltd, considering the insulation resistance tester and the experimental circumstances. To measure the temperature change, a K - type thermocouple was attached. Table 1 presents the fundamental characteristics of the varistor. Figure 3 shows the hardware composition of the leakage current and insulation resistance tests according to the temperature changes and voltage. To check the changes in leakage current and insulation resistance according to the applied voltage rise at room temperature, a voltage was sequentially applied for one minute using an insulation resistance tester. The changes in leakage currents and insulation resistance were measured by applying a voltage to the varistor while increasing the temperature sequentially using a convection oven. In the experiment, the same specimens were used to calculate the average value after three repeated measurement.

Figure 4 shows the measurement results of changes in leakage current and insulation resistance of the varistor by sequentially applying a voltage from 50 V to 477 V_{DC} at room temperature. In the pre-breakdown region below around 400 V_{DC}, resistance decreases as voltage increases, whereas the leakage current increases proportionally. In the breakdown and upturn regions above around 470 V_{DC},

TABLE 1. Electric specifications of TVR-14471.

Model No.	Dimension	Varistor voltage (1 mA)	Maximum operating voltage		Maximum surge current (8/20 μs)
TVR-14471-D	14 mm	470 V_{DC}	V_{AC}(rms) 300 V	V_{DC} 385 V	4.5 kA

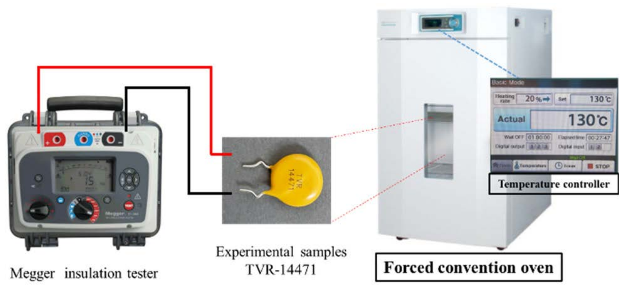

FIGURE 3. Hardware composition.

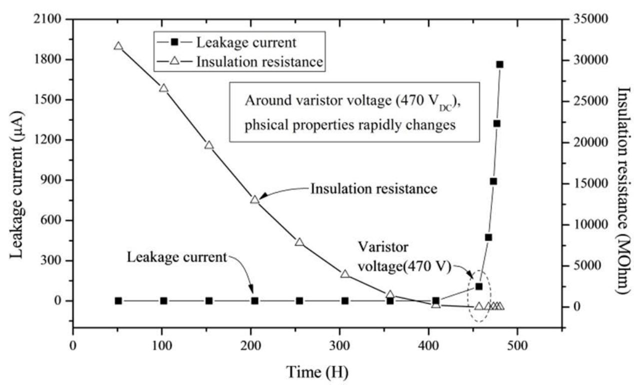

FIGURE 4. Current–voltage characteristics of TVR-14471-D.

insulation resistance rapidly decreases, and the leakage current rapidly increases. This verifies that the varistor changes from an insulation status to a short circuit.

Figure 5 shows the physical properties of the varistor according to changes in the external environment (temperature rise). A varistor was installed inside the convection oven, and the temperature increased from 20°C to 40°C, 60°C, 80°C, 100°C, 120°C, 140°C, and 160°C to measure changes in leakage current and insulation resistance accordingly. Figures 5(a) and (b) verify an increase in leakage current and a reduction in the insulator's resistance as the temperature increases. In addition, it verifies decreasing insulation resistance of the varistor at 100°C or higher, and even below the V_N, a leakage current gradually increased. This indicates that heating may be generated by a leakage current, but deterioration may also be accelerated, depending on the place where the SPD is applied. Figure 5(c) verifies that a change in the leakage current does not occur rapidly as the temperature increases in voltage below 400 V_{DC}, whereas the leakage current increases rapidly as the voltage is closer

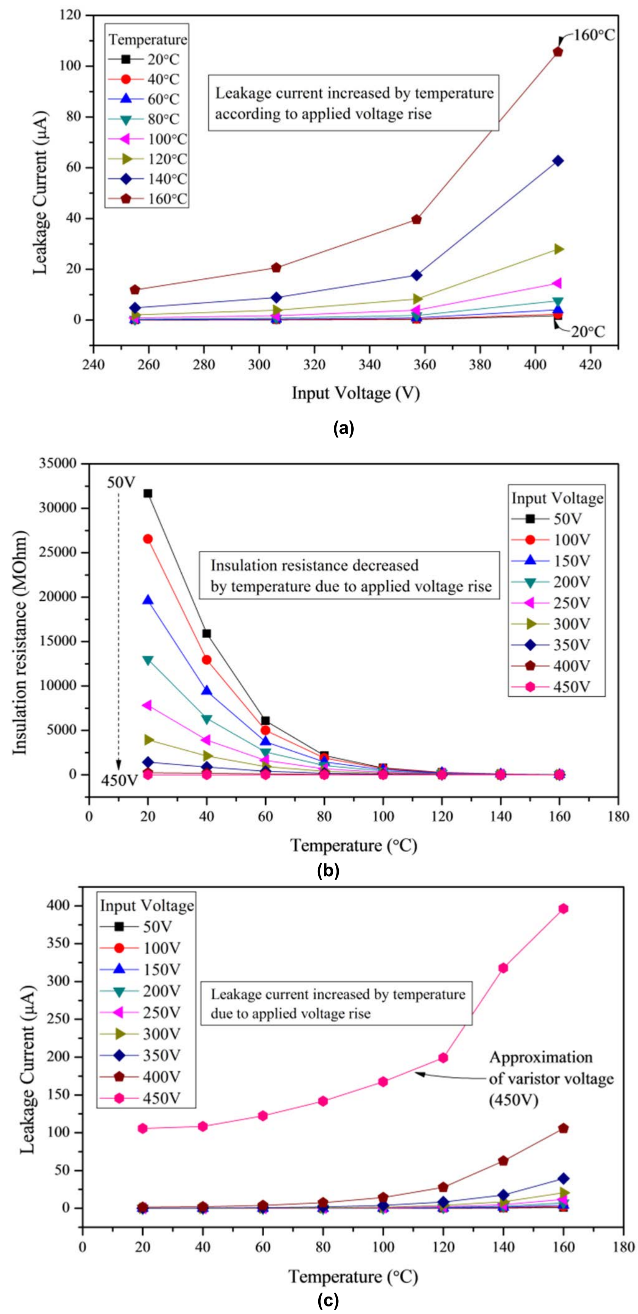

FIGURE 5. Physical properties of TVR-14471–D with increasing temperature (a) Leakage current by temperature according to applied voltage rise (b) Insulation resistance change according to temperature rise (c) Leakage current change due to temperature rise.

to the V_N because the change in leakage current sensitively reacts to temperature.

To verify the effect of the deterioration of the varistor on the failure mechanism, accelerated aging tests were conducted to evaluate the insulation resistance and leakage current of the varistor. Figure 6 shows the experimental results to verify the change in physical properties due to heating caused by the leakage current that flows in the varistor. To artificially deteriorate the varistor at an accelerating rate, heating was

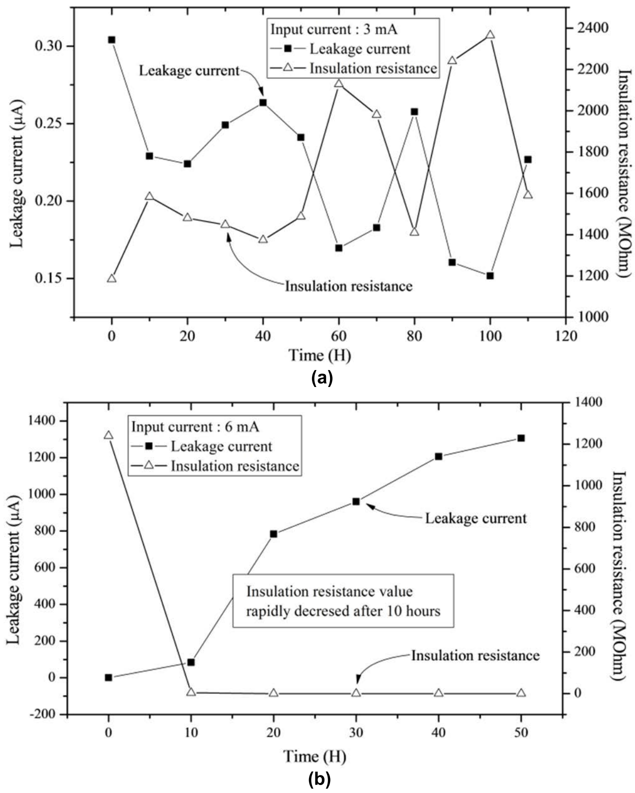

FIGURE 6. **Leakage current characteristics of varistor according to deterioration time (a) Characteristics of leakage current and insulation resistance (500 V applied) (b) Characteristics of leakage current and insulation resistance (520 V applied).**

generated in a region (500 V_{DC}: 3 mA, 520 V_{DC}: 6 mA) with conduction status. After the continuous application for 10 hours, the voltage was turned off (0 mA of leakage current) to drop the temperature to room temperature, and then 370 V_{DC}, which was lower than the maximum operating voltage (Uc), was applied to check whether the varistor failed. Figure 6(a) shows the experimental result in which a voltage of 500 V_{DC} was applied where the leakage current was 3 mA, and the varistor temperature caused by the leakage current increased to around 100°C. Despite the fact that a minimal change in leakage current and insulation resistance value was observed for 110 hours, failure did not occur. On the other hand, the insulation resistance value rapidly decreased after 10 hours at a voltage of 520 V_{DC} (6 mA of leakage current: around 150°C), and the leakage current increased over time, as verified in Figure 6(b). This implies that the level of heating varies according to the size of the current flowing in the varistor caused by the inflow of abnormal voltage. In addition, changes in the physical properties occur due to heat accumulation, thereby degrading performance and resulting in the possible malfunction of the varistor.

IV. OPERATING DUTY TEST OF VARISTOR

An operating duty test was conducted to check the operating characteristics of the varistor inside the SPD. The operating duty test was performed according to IEC 61643 - 11, and it started while applying the maximum continuous Uc of the SPD [27]. The varistor should have no abnormal functions and should have resistance to discharge current as well as thermal stability. Thermal stability refers to a thermal characteristic in which the SPD temperature decreases over time when applying the designated Uc after the operating duty test, which causes a temperature rise. Several surge impulses were applied to the SPD while supplying a Uc alternating current (AC) power source. The power supply was connected to the varistor, and impulses were synchronized with the frequency of the power supply to increase the phase angle from 0° to an increment of 30°, applying Uc 15 times. The operating duty test was divided into Type II and Type I. Type I aimed to prevent damage due to lightning stroke at the installation point of the internal lightning protection system, in which the maximum value of lightning impulse current (limp) in the 8/20 μs current waveform was applied. In the Type II SPD test, an SPD was installed when the failure probability of the SPD was ignored, as a lead-in wire was located inside the lightning area rather than a complete direct lightning strike area, in which the maximum value of the nominal discharge current (In) in the 8/20 μs current waveform was applied. Based on the above, a test was conducted, and the applied surge current was set based on the maximum surge current (1.84 kA, 3.94 kA, and 7.1 kA) to apply to the varistor.

A direct lightning strike surge current generator, which was designed and manufactured according to Institute of Electrical and Electronics Engineers (IEEE) and Underwriters' Laboratories (UL) standards, was employed. Figure 7 shows the configuration of the experimental device and circuit diagram [28], [29], [30], [32], [33], [34]. The maximum Uc (300 V_{rms}) of the varistor TVR - 14471 was applied. Based on the maximum ln value (4.5 kA) of the 8/20 μs current waveform, a test was conducted by dividing the current into 7 kA, 4 kA, and 2 kA in the Type II SPD test using a lightning impulse current generator and a high-voltage differential probe. As shown in Figure 7, a four-channel oscilloscope (MSO44) was used to measure the current, and then the current was converted to be calculated using a Rogowski current waveform transducer (CWT1500B).

The physical properties of the varistor due to changes in voltage and external environments were tested using an insulation resistance tester and convection oven based on the samples used in the previous test to evaluate thermal stability.

To check the change in the varistor according to surge size and count, the temperature inside the convection oven was set to 20°C, 40°C, 60°C, 80°C, 100°C, 120°C, 140°C, and 160°C to observe the changes in leakage current and insulation resistance by applying the V_N.

A. PRELIMINARY TEST

Table 2 presents the results of the operating duty test of the varistor according to the impulse current. In this test, changes in the V_N applied to both ends of the varistor were checked when applying 1 mA using a multi tester. The pass or failure

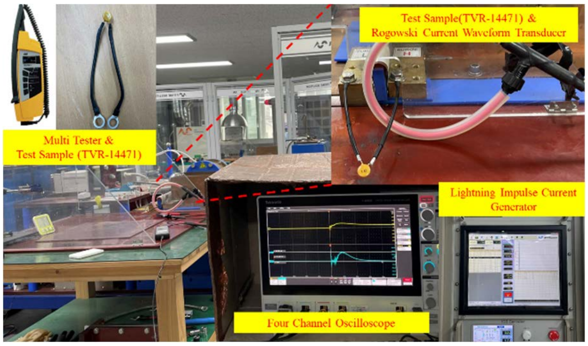

(a)

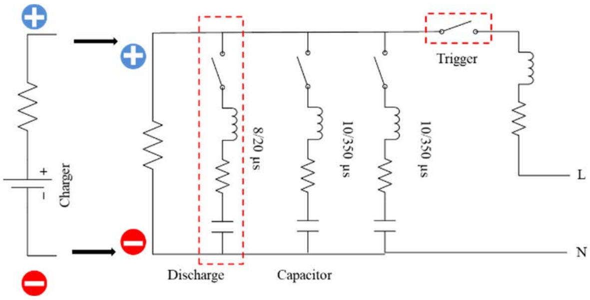

(b)

FIGURE 7. **Configuration of lightning impulse current test (a) Composition of operating duty test (b) Circuit diagram of lightning impulse current generator.**

was evaluated according to Table 4 - General pass criteria of the design test in IEC 61643 - 11. The varistor samples, where 5 times, 10 times, and 15 times of 1.85 kA were applied, had minimal changes in V_N, and the operating duty test was determined to have passed. This meant that the maximum surge current of the TVR - 14471 sample was 4.5 kA, which did not have a significant impact on performance (Survey of Damage Cases for Surge Protective Devices Installed Electrical Communication Systems and Analysis of Degradation Diagnosis Method). As the number of applying 3.85 kA increased, the change in V_N also increased (6 - 12 V), and it was determined to have failed in the operating duty test. The varistor sample, where 7.1 kA was applied once, showed a significant decrease from 491 V to 436 V. It was determined to have failed in the operating duty test, which was expected, as there was a performance difference according to a change in the physical properties. Figure 8 shows the sample used in the test, where twice of 7.1 kA and 12 times of 3.94 kA were applied. The sample was damaged during the test. Since the max surge current was 4.5 kA, it exceeded the performance limit. Thus, we determined that the grain boundary of the varistor was damaged.

B. EXPERIMENTAL RESULTS

Figure 9(a) shows the fundamental surge current waveform, which is determined by the wavefront and wavetail times and the peak value of the current [27], [28]. The points corresponding to 10% and 90% of the peak values in the current rise portion are connected to a line, the virtual origin point is set to a portion where the line meets the x-axis (time), and the endpoint is set to a portion where the virtual line and the peak value meet. A portion where 50% of the peak value and the current waveform meet is marked. The steepness of the wavefront refers to an indication of a rapid rise in voltage and current. The wave peak time refers to the level of voltage and current rise. The wavetail time refers to the duration of the shock wave. In the graph, the wavefront time is a time from F to J, and the wavetail time is a time from F to K. Figure 9(b) shows the current waveform measured in the operating duty test. This is expressed similarly to that in Figure 9(a). Which verifies that the test was conducted in the 8/20 μs, SPD Type II test conditions.

Figure 10 shows the changes according to the number of 2 kA lightning impulse currents (5, 10, and 15 times) applied caused by changes in abnormal voltage and external

TABLE 2. **Results of operating duty test.**

TEST	V_{NI}	V_N	PASSED OR FAILED
7.1 kA once applied	491	436	FAILED
3.94 kA once applied	499	493	FAILED
3.94 kA three times applied	495	484	FAILED
3.94 kA Five times applied	490	478	FAILED
3.94 kA 10 times applied	476	449	FAILED
1.84 kA 5 times applied	496	501	PASSED
1.84 kA 10 times applied	498	505	PASSED
1.84 kA 15 times applied	486	495	PASSED

FIGURE 8. **Photographs of the test samples.**

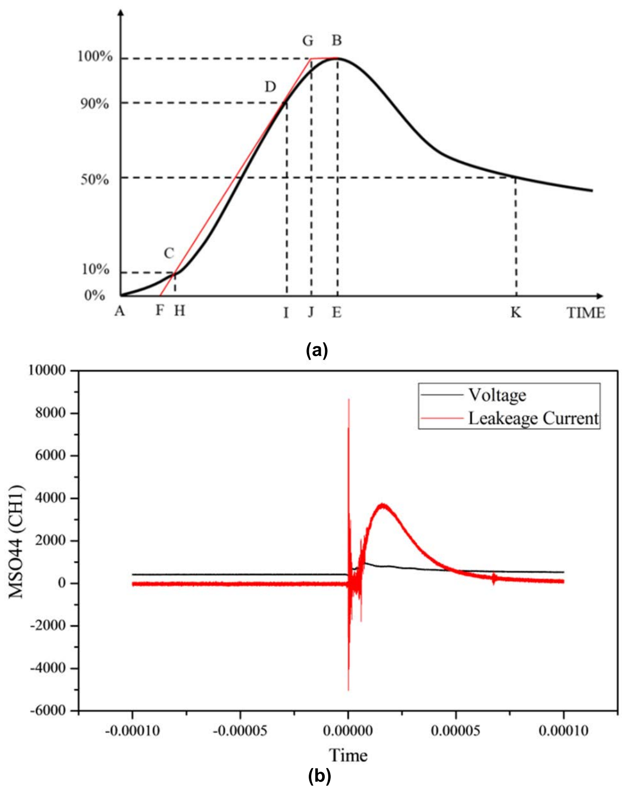

FIGURE 9. The waveform of the operating duty test (a) Fundamental surge current waveform (b) surge waveform measured during operating duty test.

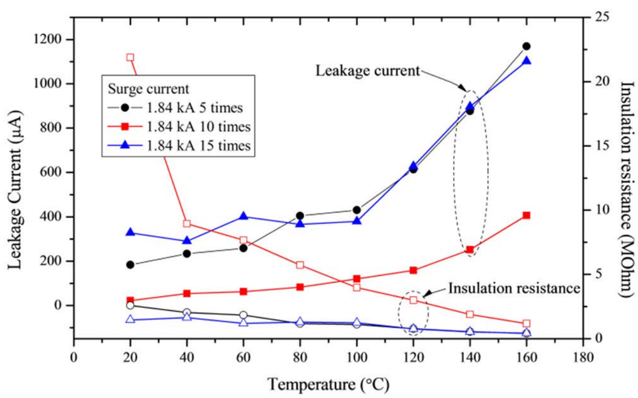

FIGURE 10. Leakage current and insulation resistance characteristics by the number of surge currents applied (1.84 kA).

environments in the operating duty test. It shows a trend of an increase in leakage current and decreases in insulation resistance as the temperature rises, but no significant difference is shown in changes as the number of currents applied increases. Since the maximum surge current of TVR - 14471 was 4.5 kA, the change in V_N was minimal, as presented in Table 2. Accordingly, the damage to grain boundary of the varistor was insignificant and did not have a significant impact on performance degradation.

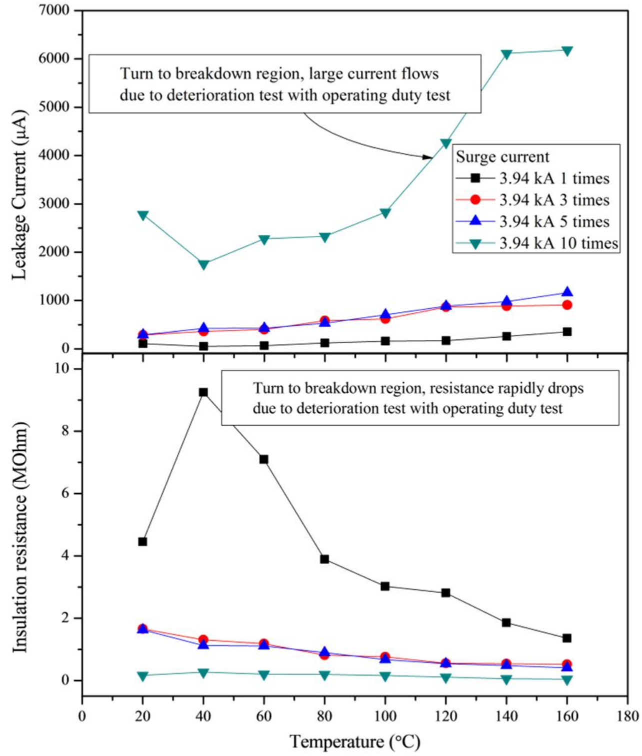

FIGURE 11. Leakage current and insulation resistance characteristics by the number of surge currents applied (3.94 kA).

Figure 11 shows the changes according to the number of 4 kA lightning impulse currents applied caused by changes in abnormal voltage and external environments in the operating duty test. The varistor that absorbed a 4 kA surge was determined to have failed in the operating duty test. The deterioration test using an insulation resistance tester shows a trend of increasing leakage current and decreasing insulation resistance as the temperature rises. As the number of surge currents applied increased, the leakage current of the sample where the surge current was applied increased, and insulation resistance decreased. In particular, changes in the leakage current and insulation resistance of a sample where 3.94 kA was applied 10 times were around 30% of a sample where 3.94 kA was applied once. Considering that the maximum surge current of TVR - 14471 was 4.5 kA, the change in V_N was found to be around 6 - 2 V, as presented in Table 2, which was determined as a section that affected the performance degradation due to the occurrence of damage to the grain boundary of the varistor.

Figure 12 shows the changes according to the number of 7 kA lightning impulse currents applied caused by changes in abnormal voltage and external environments in the operating duty test. The varistor was determined to have failed in the operating duty test. It was damaged in most tests when an impulse current was applied. The deterioration test results through the changes in V_N applied and external environments exhibited a trend of increasing leakage current and decreasing insulation resistance as the temperature rose. This showed a

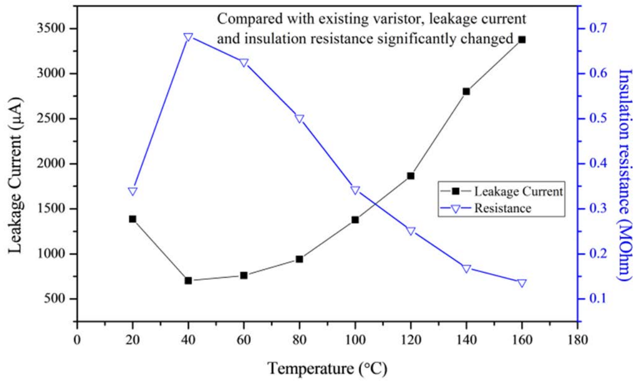

FIGURE 12. Leakage current and insulation resistance characteristics by the number of surge currents applied (7.1 kA).

significantly increased leakage current compared to that of the existing varistor. Considering that the maximum surge current of TVR - 14471 was 4.5 kA, the grain boundary inside the varistor was destroyed when a 7 kA surge current was applied, which led to damage. This meant that when an impulse current that exceeded the maximum surge current was applied, the change in V_N deepened as the number of currents applied increased. Accordingly, it caused damage to the grain boundary of the varistor, resulting in changes in the physical properties and performance degradation, which may lead to destruction and damage to the varistor.

V. CONCLUSION

Although the deterioration of SPDs, which are used to prevent electric disasters caused by a lightning flash to earth, can induce fire accidents, in-depth studies have not been conducted on this phenomenon, and only a few methods of quantitatively proposing a cause of the fire and a replacement cycle have been found. The physical performance of a varistor, which is a protective element of SPD, changes according to environmental conditions. In this study, fundamental physical properties were analyzed using a voltage applied and temperature change using an insulation resistance tester. As voltages applied to a varistor and external temperature rose, the leakage current increased, and insulation resistance decreased. As the temperature became high, the deviation of the increase in leak-age current deepened further. In particular, the leakage current rose significantly according to temperature, even under V_N. As a result, heating was generated, and heat was accumulated. This meant that heating and deterioration accelerated due to the leakage current, depending on the place where the SPD was applied. An accelerated aging test was conducted to verify the relationship between the level of deterioration in a varistor and the failure mechanism. The measured heating in the varistor where 500 V (3 mA) was applied for 110 hours was 100°C, but the change in the leakage current and insulation resistance was minimal, which did not lead to failure. The measured heating in the varistor where 520 V (6 mA) was applied was 150°C. The insulation resistance dropped rapidly after 10 hours, and the leakage current increased. This indicated that the performance may be degraded accordingly, which may lead to the failure of the varistor.

We verified the changes in the leakage current and insulation resistance due to the changes in surge current applied and the external environment through the operating duty test. The changes in the physical properties of the varistor where 1.84 kA was applied 5, 10, and 15 times were minimal. The leakage current of the varistor where 3.94 kA was applied increased, and the insulation resistance decreased as the number of surge currents applied increased from once to 3, 5, and 10 times. In particular, the increase in leakage current and decrease in insulation resistance of the varistor where the number of surge currents applied was 10 times were significant. We also verified that the varistor where 7.1 kA was applied once had a significant increase in leakage current and a decrease in insulation resistance compared to the existing varistor. This indicated that changes in the physical properties occurred due to a surge current followed by heating and heat accumulation caused by damage to the grain boundary, leading to a failure of the varistor. Furthermore, it can cause a fire if it affects nearby combustibles. Thus, it is necessary to identify the mechanism by which a leakage current flows through the analysis of the deterioration characteristics and grain in a varistor and to conduct additional studies that can propose a replacement cycle.

REFERENCES

[1] C. Price, "Thunderstorms, lightning and climate change," in *Lightning: Principles, Instruments and Applications*, H. D. Betz, U. Schumann, and P. Laroche, Eds. Dordrecht, The Netherlands: Springer, 2009, pp. 521–535, doi: 10.1007/978-1-4020-9079-0_24.

[2] *Protection Against Lightning—Part 1: General Principles*, document IEC 62305-1, Int. Electrotechnical Commission, Geneva, Switzerland, 2004.

[3] R. L. Cohen, *How to Protect Your House and its Contents From Lightning, IEEE Guide for Surge Protection of Equipment Connected to AC Power and Communication Circuits*. Piscataway, NJ, USA: IEEE Press, 2005.

[4] *National Fire Data System*, Nat. Fire Agency, Sejong, South Korea, 2021. [Online]. Available: https://www.nfds.go.kr

[5] I. M. Y. Negara, D. Fahmi, D. A. Asfani, I. S. Hernanda, R. B. Pratama, and A. B. Ksatria, "Investigation and improvement of standard external lightning protection system: Industrial case study," *Energies*, vol. 14, no. 14, p. 4118, Jul. 2021, doi: 10.3390/en14144118.

[6] *Protection Against Lightning—Part 2: Risk Management*, document IEC 62305-2, Int. Electrotechnical Commission, Geneva, Switzerland, 2010.

[7] *Protection Against Lightning—Part 3: Physical Damage to Structures and Hazard*, document IEC62305-3, International Electrotechnical Commission, Geneva, Switzerland, 2010.

[8] *Protection Against Lightning—Part 4: Electrical and Electronic System Within Structures*, document IEC 62305-4, Int. Electrotechnical Commission, Geneva, Switzerland, 2003.

[9] K. H. Lee, "Current status and cases of lightning damages in Korea," in *Proc. KIIEE*, Sejong, South Korea, 2007, pp. 45–47.

[10] S.-D. Kang, S.-C. Kim, K.-B. Park, and J.-H. Kim, "A study on the current status and reduction method caused by lightning at educational facilities," *Energies*, vol. 14, no. 11, p. 3015, May 2021, doi: 10.3390/en14113015.

[11] J. He, Z. Yuan, J. Xu, S. Chen, J. Zou, and R. Zeng, "Evaluation of the effective protection distance of low-voltage SPD to equipment," *IEEE Trans. Power Del.*, vol. 20, no. 1, pp. 123–130, Jan. 2005.

[12] G. B. Lo Piparo, R. Pomponi, T. Kisielewicz, C. Mazzetti, and A. Rousseau, "Protection against lightning overvoltages: Approach and tool for surge protective devices selection," *Electr. Power Syst. Res.*, vol. 188, Nov. 2020, Art. no. 106531, doi: 10.1016/j.epsr.2020.106531.

[13] T. H. Kuan, K. W. Chew, and K. H. Chua, "Practical approach on surge protection device for Ex application," in *Proc. 1st Int. Conf. Electr., Control Instrum. Eng. (ICECIE)*, Nov. 2019, pp. 1–7, doi: 10.1109/ICECIE47765.2019.8974781.

[14] J.-C. Kim, J.-S. Jeon, C.-O. Ki, G.-R. Choi, and S.-J. Lee, "Protection of MOV thermal runaway and safety improvement of SPD using built-in instantaneous trip device," *J. Korean Inst. Illum. Electr. Installation Eng.*, vol. 25, no. 2, pp. 120–125, Feb. 2011.

[15] A. Rousseau and F. Cruz, "Surge protective devices standards," presented at the ILPS, Shenzhen, China, Oct. 2018.

[16] *Low-Voltage Surge Protective Devices—Part 12: Surge Protective Devices Connected to Low-Voltage Power Distribution Systems-Selection and Application Principles-Requirements and Test Methods*, document IEC61643-12, International Electrotechnical Commission, 2012.

[17] C. Li, C. Zhang, G. Zhang, M. Kong, and Z. Yang, "Analysis of the failure mode of surge protector under multi-pulse lightning strikes and its mechanism," *Energy Rep.*, vol. 8, no. 13, pp. 487–497, Nov. 2022, doi: 10.1016/j.egyr.2022.08.065.

[18] H. Ito, K. Terashima, and S. Yun, "Two case studies on energy and protection level coordination of an SPD system," in *Proc. Int. Conf. Lightning Protection (ICLP)*, Oct. 2014, pp. 1064–1069, doi: 10.1109/ICLP.2014.6973282.

[19] C. Zhang, X. Yi, C. Li, G. Zhang, and M. Kong, "Study on lightning thermal damage characteristics of ZnO varistor under operating duty," in *Proc. IEEE Asia–Pacific Conf. Image Process., Electron. Comput. (IPEC)*, Apr. 2022, pp. 982–985, doi: 10.1109/IPEC54454.2022.9777496.

[20] Y. He, J. Liu, Y. Zhu, and Z. Fu, "Withstand performance of SPD varistor under multi-waveform multi-pulse currents," in *Proc. ISH*, 2019, pp. 1197–1204, doi: 10.1007/978-3-030-31680-8_114.

[21] J. W. Lim, J. Y. Lee, and J. H. Kwon, "Survey of damage cases for surge protective devices installed electrical communication systems and analysis of degradation diagnosis method," in *Proc. Conf. KIITFE*, Sejong, South Korea, 2009, pp. 15–18.

[22] T. Kisielewicz, G. B. L. Piparo, and C. Mazzetti, "Surge protective devices efficiency for apparatus protection in front of direct flashes to overhead low voltage lines," *Electr. Power Syst. Res.*, vol. 134, pp. 88–96, May 2016, doi: 10.1016/j.epsr.2016.01.008.

[23] D. R. Clarke, "Varistor ceramics," *J. Amer. Ceram. Soc*, vol. 82, no. 3, pp. 485–502, 1999.

[24] M. A. Alim, S. Li, F. Liu, and P. Cheng, "Electrical barriers in the ZnO varistor grain boundaries," *Phys. Status Solidi A*, vol. 203, no. 2, pp. 410–427, Feb. 2006.

[25] E. Olsson and L. K. L. Falk, "The microstructure of a ZnO varistor material," *J. Mater. Sci.*, vol. 20, no. 11, pp. 4091–4098, Nov. 1985.

[26] S. Hirose, K. Nishita, and H. Niimi, "Influence of distribution of additives on electrical potential barrier at grain boundaries in ZnO-based multilayered chip varistor," *J. Appl. Phys.*, vol. 100, no. 8, Oct. 2006, Art. no. 083706.

[27] *Low-Voltage Surge Protective Devices—Part 11: Surge Protective Devices Connected to Low-Voltage Power Systems-Requirements and Test Methods*, document IEC61643-11, International Electrotechnical Commission, 2011.

[28] *IEEE Standard Techniques for High-Voltage Testing*, IEEE Standard 4, 1–135, Oct. 12, 1995, doi: 10.1109/IEEESTD.1995.81695.

[29] *IEEE Recommended Practice on Characterization of Surges in Low-Voltage (1000 V and less) AC Power Circuits*, IEEE Standard C62.41.2-2002, Apr. 11, 2003, pp. 1–52, doi: 10.1109/IEEESTD.2003.94254.

[30] *IEEE Recommended Practice on Surge Testing for Equipment Connected to Low-Voltage (1000 V and less) AC Power Circuits*, IEEE Standard C62.45-2002 (Revision of IEEE Std C62.45-1992), Apr. 11, 2003, pp. 1–96, doi: 10.1109/IEEESTD.2003.94255.

[31] *IEEE Guide on Interactions Between Power System Disturbances and Surge Protective Devices*, IEEE Standard C62.48-2005 (Revision of IEEE Std C62.48-1995), Nov. 11, 2005, pp. 1–26, doi: 10.1109/IEEESTD.2005.97888.

[32] *IEEE Standard Test Specifications for Surge-Protective Devices (SPDs) for Use on the Load Side of the Service Equipment in Low Voltage (1000 V and less) AC Power Circuits*, IEEE Standard C62.62-2010 (Revision of IEEE Std C62.62-2000), Mar. 11, 2011, pp. 1–60, doi: 10.1109/IEEESTD.2011.5729665.

[33] *Installation Requirements for Lightning Protection Systems*, UL Standard 96A, Edition 13, Mar. 2016.

[34] M. K. Sanders, "NFPA 780 standard for the installation of lightning protection systems 2011 edition," in *Proc. IEEE Ind. Commercial Power Syst. Tech. Conf.*, May 2011, pp. 1–4, doi: 10.1109/ICPS.2011.5890891.

AHRAN MIN received the B.S. degree in fire and disaster prevention from the University of Daejeon, in 2021. She is currently pursuing the M.S. degree in fire and disaster prevention with Daejeon University.

SIN-DONG KANG received the M.S. degree in fire and disaster prevention from the University of Daejeon, in 2019. He is currently pursuing the Ph.D. degree in fire and disaster prevention with Daejeon University.

JAE-HO KIM received the Ph.D. degree in electrical engineering from Changwon National University, in 2010. He was a Postdoctoral Researcher at the Center for Advanced Power Systems (CAPS), Florida State University, from 2009 to 2012. Since March 2012, he has been a Professor with the School of Fire and Disaster Prevention, Daejeon University, Daejeon, South Korea. His research interests include life assessment, superconducting cable, fire protection, and electrical safety.